doi: 10.15407/ujpe61.03.0240

V.A. VINICHENKO, V.V. BUCHENKO, N.S. GOLOBORODKO, V.V. LENDEL, A.E. LUSHKIN, V.N. TELEGA

Taras Shevchenko National University of Kyiv, Faculty of Physics
(64/13, Volodymyrs'ka Str., Kyiv 01601, Ukraine; e-mail: vbuchenko@yandex.ua)

PACS 68.37 Hk, 68.55.-a, 78.40.-q, 78.66.–w

OPTICAL AND ELECTROPHYSICAL PROPERTIES OF 95% $In_2O_3 + 5\%$ SnO_2/ns-Si HETEROSTRUCTURE

Optical and electrical properties of 95% In_2O_3 + 5% SnO_2/ns-Si heterostructures with films 6 and 12 nm in thickness deposited on a nanostructured silicon surface by the magnetron sputtering have been considered. It is shown that the 6-nm film is characterized by several peaks in the optical absorption spectrum, while the 12-nm film has no absorption peaks in the same spectral interval. The influence of the environment and the optical irradiation on the electrical properties of 95% In_2O_3 + 5% SnO_2/ns-Si structures is determined. Their response to the gas environment is shown to be governed by the dielectric permittivity of an adsorbate. The results obtained can be used in the development of resistive gas sensors based on 95% In_2O_3 + 5% SnO_2/ns-Si films.

Keywords: current-voltage characteristics, absorption spectrum, thin films, transparent oxides.

1. Introduction

Owing to their electrophysical properties, metal oxides find a wide application in modern electronics, in particular, for the production of solar cells and transparent electrodes for them, electroluminescent light-emitting diodes, and gas sensors [1–7]. Metal oxides that are used in electronics are wide-band-gap semiconductors. Among the materials of this kind, the most widespread are SnO_2 and In_2O_3 [8–10]. Those materials have got popularity, in particular, in the manufacture of film gas sensors [2, 10–13].

For the functioning of devices created on the basis of indium and tin oxide films, their electric and optical parameters such as the conductivity [10] and the optical absorption spectrum [12] are very important. Plenty of various factors, both external and internal, can affect them. As an example, various impurities are often inserted in order to control the conductivity of oxide films. For instance, to modify the conductivity and sensitivity of a SnO_2 sensor film in gas sensors, the film is doped with such substances as In_2O_3, Fe_2O_3, Sb, ZrO_2, and SiO_2 [13]. Doping makes it possible to reduce the working temperature of a sensor and to enhance its selectivity. It is worth noting that, while studying the electrophysical properties of structures on the basis of metal oxides, in particular, current-voltage characteristics (CVCs), the branch of reverse currents is often studied, because the influence of external factors reveals itself better at low currents [14–16].

Among metal oxide composites, the composite of indium and tin oxides (ITO) got a wide application [1, 17]. Moreover, by varying the component content in this composite, it is possible to change its electrophysical properties. For instance, the authors of work [1] showed that the ITO films with a content of 90% $In_2O_3 + 10\%$ SnO_2 have the highest conductivity and strongly absorb light in the infra-red spectral interval in comparison with films with other possible contents.

On the other hand, the conductivity of the films concerned is affected by the concentration of surface states [2]. In work [18], it was shown that if a SnO_2 film is deposited onto a substrate fabricated of porous silicon, the surface states with an energy of about 2 eV with respect to the valence band top stimulate the electroluminescence of those structures in the visible spectral interval. The authors of work [19] showed that the application of the porous silicon substrate allows the room-temperature sensitivity of a sensor on the basis of a SnO_2 film to be considerably enhanced.

In works [12, 14], it was shown that the irradiation of porous SiO_2 increases its conductivity. However, the influence of light on the electrophysical properties of heterostructures consisting of ITO films deposited on porous silicon substrates still remains insufficiently studied. Considering the optical properties of ITO films [1], we may suppose that their illumination with light can increase the conductivity of heterostructures on their basis. This work was aimed at studying the influence of the environment and the ITO film thickness on the optical and electrophysical properties of 95% $In_2O_3 + 5\%$ SnO_2/ns-Si heterostructures.

2. Experimental Technique

2.1. Experimental specimens

ITO films with a composition of 95% $In_2O_3 +$ $+ 5\%$ SnO_2 were deposited onto *p*-silicon wafers of the KDB-7.5 grade with the orientation (100) and a thickness of 200 μm. Before the film deposition, the silicon surface was subjected to the texturing treatment:

• nanostructuring of the silicon surface by the chemical etching in a 2% aqueous solution of KOH and a 4% aqueous solution of isopropyl alcohol at a temperature of 75°C for 10 min;

• etching in the mixture $HCl : H_2O_2 : H_2O$ (taken in a ratio of 1 : 1 : 5) at 90 °C for 10 min to get rid of KOH alkali, washing in deionized water, etching in a 1% solution of fluoric acid (HF) for 30–40 s, washing in deionized water, boiling in the peroxide-ammonia solution $H_2O_2 : NH_4OH : H_2O$ (taken in a ratio of 1 : 1 : 5) at 90 °C for 10 min, treatment in a 1% solution of fluoric acid for 30–40 s, and washing in deionized water;

• oxidation at 1000 °C in a diffusion furnace SDOM-3M in the dry (15 min), damp (45 min), and dry again atmosphere;

• protection of one side of the specimen by a photoresist;

• etching in the buffer etching solution $NH_4F : HF : H_2O$ (taken in a ratio of 1 : 1 : 20) at 90 °C for 10 min;

• removal of a photoresist, washing in deionized water, the diffusion of boron from a solid source at a temperature of 920 °C for 40 min (driving-in) and at 1050 °C for 2 h (driving-away);

• glass and oxide etching in a 5% solution of HF;

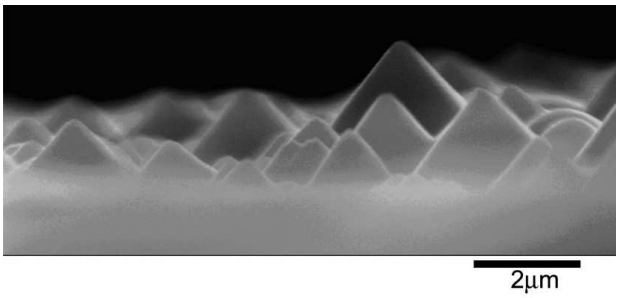

a

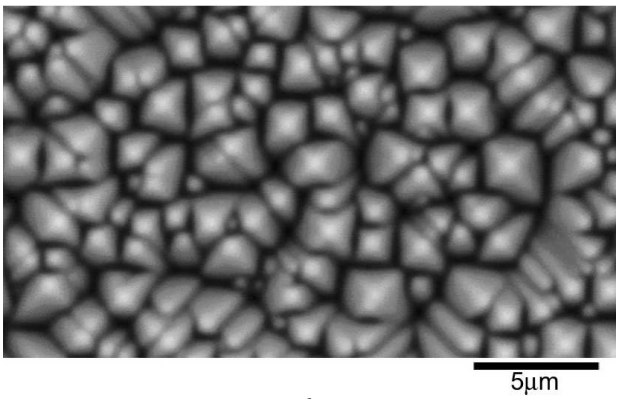

b

Fig. 1. SEM image of a textured silicon surface

• sputtering of an aluminum film to a thickness of 500 nm at 125 °C on a vacuum sputtering installation Katod-1M;

• annealing at 510 °C for 15 min in a nitrogen flow in a diffusion furnace to form ohmic contacts;

• sputtering of a Ti–M0–Ag layer to a thickness not exceeding 500 nm.

In Fig. 1, the scanning electron microscopy image of the silicon substrate surface is shown. One can see that the specimens have a textured surface rather than a smooth one. The height of pyramids on this surface equals 1–5 μm. When nanostructured silicon is formed on a single-crystalline silicon substrate, not only its structural properties change, which results in the variation of the energy gap width and the appearance of quantum-size effects [20], but also new silicon compounds with an increased content of hydrogen and amorphous silicon are formed on the surface [21]. Such a complicated structure favors the manifestation of new properties associated with the light scattering by inhomogeneities in the medium [22, 23].

ITO films were sputtered on a modernized installation VUP-5 for vacuum sputtering using the method

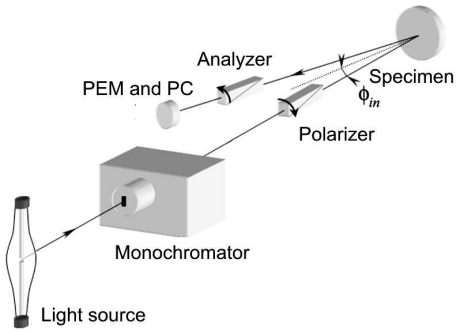

Fig. 2. Block diagram of the installation for spectroscopic ellipsometry researches

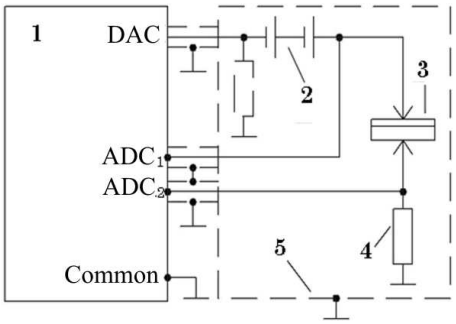

Fig. 3. Scheme of the unit for measuring CVCs of experimental specimens

of dc magnetron reactive sputtering of a metal target fabricated from InO-5 alloy (5 wt.% Sn + 95 wt.% In) in the discharge of a gas mixture consisting of argon and oxygen taken in a volume fraction of 2 : 1. Before the sputtering, the substrates were treated in a 5% solution of HF for 30 s. The installation chamber was preliminarily evacuated to a pressure of $(2 \div 3) \times \times 10^{-5}$ Torr. Then the gas mixture was let into the chamber to a pressure of 7×10^{-3} Torr. The distance from the target to the substrate was 45 mm, the discharge current amounted to 200 mA, and the film thickness was 6 or 12 nm.

Silver contacts to ITO films were sputtered on the same installation (VUP-5), by using the method of thermal evaporation from a molybdenum boat 500 nm in thickness through a magnetic mask.

2.2. Absorption measurement unit

The block diagram of experimental installation with a spectral ellipsometer is depicted in Fig. 2 [24]. A halogen incandescent lamp was used as a light source. In the installation, we used a monochromator DMR-4 with interchangeable glass and quartz optic units. Specimens were mounted on a goniometer together with an analyzer and a photoelectronic amplifier (PEM) FEU-100. The latter was used to register signals. After the PEM, the signal was amplified with the help of an ac amplifier and, after being detected by a synchronous detector, was registered by a digital voltmeter V7-21.

The errors of optical constants are determined by the accuracy of dials used to measure the incidence angle and the polarizer and analyzer azimuths, as well as by the intensity measurement error. The relative determination error for ellipsometric parameters equals [25]

$$\tan\psi\, e^{i\Delta} = \frac{R_p}{R_s}, \tag{1}$$

where R_p and R_s are the Fresnel amplitude reflection coefficients. The measurement errors for ellipsometric parameters were $\delta\psi/\psi \approx 1\%$ and $\delta\Delta/\Delta \approx 1.5\%$.

The spectral dependences were measured in air at room temperature.

2.3. CVC measurement unit

To measure the current-voltage characteristics and to observe their variations under the influence of various gas environments, we used an original device (Fig. 3) created on the basis of interface board 1 containing high-rate (a conversion time of 8 μs) 12-bit analog-to-digital converters (ADCs) and a sweep generator, the role of which was played by one of the channels of a 12-bit double-buffered digital-to-analog converter (DAC) with a settling time of 30 μs. The DAC channel was connected in series to a galvanic source of reference voltage 2. The resulting voltage was applied to specimen 3 and to the first ADC channel, whereas the voltage proportional the the current through measuring resistance 4 was applied to the second channel of the ADC board. Measurements could be carried out both in dark and in light in a metal box 5, which served as a screen to reduce externally induced interferences in the measurement circuit.

The influence of the gas environment was studied separately in the saturated vapors of ethyl and isopropyl alcohols, as well as in air. The exposure time in the examined gas medium was 20 min. Before the gas medium was changed, the box had been ventilated for 20 min. During the procedures of exposure

of a specimen and ventilation, the power source was disconnected from the specimen.

3. Results and Discussion

3.1. Optical properties of the films

The spectral dependences of the absorption coefficient $\alpha = 2\pi/\lambda$ measured in ITO films are depicted in Fig. 4. A characteristic feature in the behavior of the film absorption coefficient is the presence of a few absorption maxima (at 405, 467, 526, and 608 nm) for the film 6 nm in thickness. It should be noted that the corresponding absorption maxima are absent for the 12-nm film. Instead, the absorption spectrum for the latter film is characterized by a constant value in an interval of 469–650 nm. The indicated absorption maxima can arise as a result of the defect emergence in the transition layer between the ITO film and textured silicon. However, in order to elucidate why those features do not manifest themselves in the absorption spectrum of the heterostructure with the 12-nm ITO film, it is expedient to carry out additional researches.

The features in the optical properties of films with inclusions of other materials have been repeatedly discussed in the literature [26–28]. While interpreting the results of optical measurements obtained for the reflection or transmission of polarized light by multilayered structures (Fig. 5) [24], it is important to correctly choose the model which would adequately describe the process of light interaction with a specific multilayered medium.

Taking the aforesaid into account, we selected a model composed of pure layers and transient ones in between, the refractive index of which can be described in the effective medium approximation. According to the latter, the effective complex refractive index in the transient layer, $N = n + j\kappa$, is determined by the expression

$$\sum_m f_m \frac{N_m - N}{N_m + 2N} = 0, \quad \sum_m f_m = 1, \tag{2}$$

where $N_m = n_m + j\kappa_m$ and f_m are the complex refractive index and the volume fraction (the concentration), respectively, of the m-th component. In order to model the influence of transient layers on the total reflection coefficient, we used the angular dependences of ellipsometric parameters.

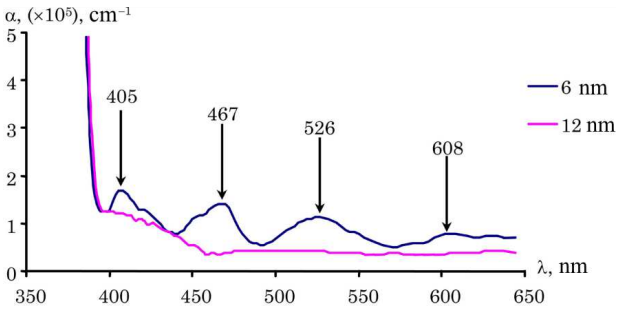

Fig. 4. Spectral dependences of the absorption coefficient α for 95% $In_2O_3 + 5\%$ SnO_2 films with various thicknesses

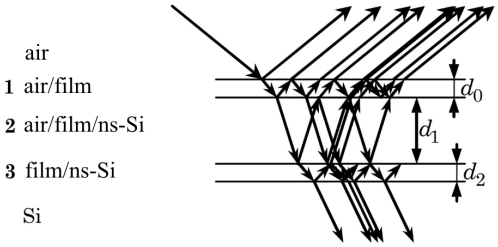

Fig. 5. Schematic illustration of the light reflection from a multilayered structure

Table 1. **Structure and content of the examined films**

Layer (Fig. 5)		6-nm film		12-nm film	
		Content, %	Thickness, nm	Content, %	Thickness, nm
1	air	99.8		99.1	
	film	0.2	3	0.9	11
2	air	53.1		53.2	
	film	2.2	2005	2.1	2007
	ns-Si	44.7		44.7	
3	film	1.6		1.4	
	ns-Si	98.4	7	98.6	13

In Table 1, the results of model calculations of parameters of the examined structures with and without interlayers are quoted. One can see that the 6-nm film is inhomogeneous across its thickness. This inhomogeneity together with a larger surface area can add new properties to the film, which are related to surface effects, because the thickness of heterojunction layers can be different at different film sites. Note also that the 12-nm film is considerably more homogeneous.

3.2. CVCs of experimental specimens

3.2.1. Influence of a gas environment

In Fig. 6, the CVC reverse branches registered for specimens with ITO films 6 and 12 nm in thickness in various gas environments are shown. It is evident that the CVCs obtained in the atmosphere of the saturated vapor of alcohols differ rather well from that registered in air.

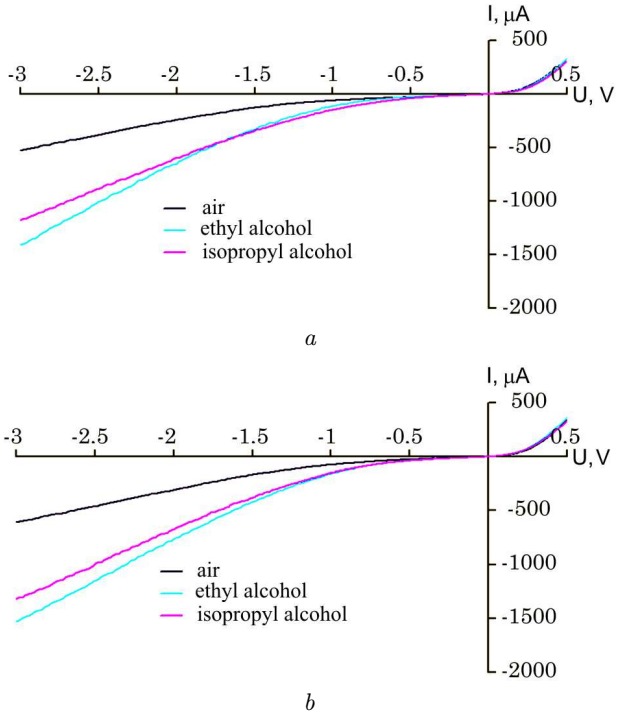

Fig. 6. CVCs for specimens with 6-nm (*a*) and 12-nm (*b*) ITO films for various gas environments

Table 2. **Dielectric permittivities ϵ of some substances [30]**

Environment	Formula	ϵ
Air	O_2+N_2	1
Isopropyl alcohol	C_3H_7OH	18.3
Ethyl alcohol	C_2H_5OH	27

Table 3. **Current at a voltage of −2.5 V**

Environment	6-nm film I, μA	12-nm film I, μA
Air	−382	−460
Isopropyl alcohol	−886	−991
Ethyl alcohol	−1023	−1145

In general, unlike our previous research [29], in which the studied specimens did not have such a developed surface, and the reverse currents for them did not exceed 200 μA, the currents for the specimens with a textured surface examined in this work are several times higher at the same voltage. This fact testifies that the latter specimens can be used as sensor structures. The growth of the response can be explained by an increase of the effective area of the working film surface.

The order, in which the obtained dependences are arranged in Fig. 6, corresponds to the values of dielectric permittivity in those substances (Table 2), which testifies that the dielectric permittivity of the adsorbate film affects the structure response to a gas environment [31].

The researched experimental specimens are complicated heterostructures, in which a superthin layer of a wide-band-gap semiconductor is located between the metal contact and silicon of the *p*-type. However, taking into account that the ITO film thickness is rather small (6 and 12 nm), the space charge region extends over the whole film thickness. As a result, the potential drop across the ITO film increases, and, consequently, the potential barrier at the metal-silicon contact decreases. Owing to the small thickness of the ITO layer, the adsorption of gases with certain dielectric permittivities gives rise to the variation of the dielectric permittivity in the near-surface layer [32]. Accordingly, the potential barrier at the metal-semiconductor interface decreases even more: the higher the dielectric permittivity of an adsorbate, the lower is the potential barrier. Defects in the transient layer between silicon and ITO can also influence the form of CVCs for the given structures [33].

From Fig. 6, one can see that the behavior of CVCs for specimens with various ITO film thicknesses is almost identical. However, the current at a reverse voltage of −2.5 V is a little higher for the 12-nm film structure in comparison with that for the 6-nm one (Table 3). Hence, from the viewpoint of obtaining the maximum sensitivity to the composition of a gas environment, the structure with the ITO layer 12 nm in thickness is more beneficial.

Note that, in order to better determine the composition of a gas environment, CVCs for the structures

concerned should be analyzed in the whole interval of measurements. Statistical methods for the analysis of integrated variations [34–36] make this task feasible.

3.2.2. Influence of illumination

There are plenty of works dealing with the influence of optical radiation on the adsorption processes and the efficiency of catalytic reactions on the surfaces of semiconductor oxides [2, 4, 6]. Note that about 0.001 of the radiation intensity is absorbed in the near-surface layer. However, this fraction can also contribute to the adsorption and desorption processes. Moreover, radiation can interact with molecules in the gas phase giving rise to their dissociation and a modification of the adsorption ability. The authors of works [37, 38] experimentally studied the influence of radiation from light-emitting diodes on the sensitivity of gas sensors on the basis of SnO_2 films obtained by the reactive magnetron sputtering onto rough quartz substrates. They analyzed the variations in the sensitivity of specimens to the vapors of ethyl and isopropyl alcohols, acetone, and benzene under their irradiation with the use of red, yellow, and blue light-emitting diodes. Actually, they showed for the first time that all forms of radiation increase the sensitivity of sensors at doses of 1–10 *ppm* for all mentioned reagents (the corresponding values equal 2–100 *ppm* in the case of low sensor sensitivity without irradiation).

In order to determine the response of structures to the optical radiation, we used light-emitting diodes (LEDs) with wavelengths of 630 nm (red), 590 nm (orange), 570 nm (yellow), 520 nm (green), and 470 nm (blue) and with a power of 1 W. The reference data were measured in dark. The CVCs of heterostructures illuminated with light with various wavelengths and registered under laboratory conditions are exhibited in Fig. 7 (the results were normalized by the minimum quantum number).

The analysis of those dependences makes it possible to say about the response growth for the structures concerned under illumination. As one can see from Fig. 7, the light waves with different lengths differently affect the response of the heterostructure with the 6-nm ITO film. Moreover, a certain correlation can be detected between the heterostructure response under illumination and the absorption coefficient at

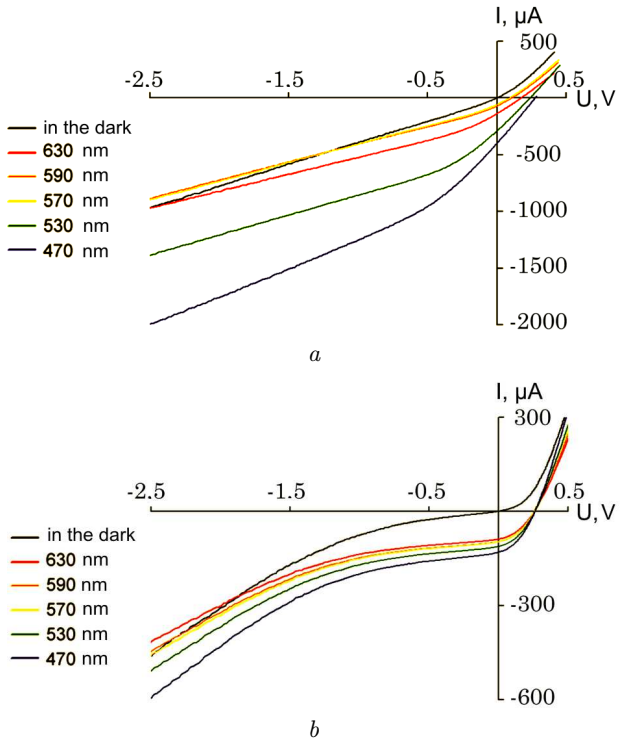

Fig. 7. CVCs for specimens with 6-nm (*a*) and 12-nm (*b*) ITO films for various wavelengths of light illumination in air

the corresponding wavelength (Fig. 4). However, an additional research of the light influence on the heterostructure with the 6-nm ITO film is required: the absorption factors for the orange (590 nm) and red (630 nm) diodes are identical within the measurement error, but Fig. 7 demonstrates that the CVC response to those diodes is substantially different. At the same time, the CVC for the illuminated heterostructure with the ITO film 12 nm in thickness changes weakly in comparison with that for the heterostructure with the 6-nm ITO film. Certainly, this is a result of a lower coefficient of absorption in this structure at the corresponding wavelengths (Fig. 4). The CVC obtained at illuminating the heterostructure with light with a wavelength of 470 nm is somewhat different from the others, because the absorption coefficient of the structure at this wavelength is a little higher than the absorption coefficient at a larger wavelength.

Note that, under the illumination, the increase in the heterostructure response should be associated with the absorption in the space charge region rather

than the intrinsic absorption in In_2O_3 or SnO_2. It is so, because the energy gap width for them is about 4 eV (300 nm), whereas the long-wave radiation limit for the radiation of a blue light-emitting diode lies at about 410 nm. In addition, it is expedient to consider the excitation of an impurity or defect centers [18], including the surface centers coupled with the adsorbent [39].

4. Conclusions

Using the method of dc magnetron reactive sputtering from a metal oxide target, a batch of 95% In_2O_3 + + 5% SnO_2/ns-Si heterostructures is created. The analysis of the current-voltage characteristics of fabricated specimens showed that the saturated vapor of alcohols affects the electric properties of examined heterostructures. A thickness of 12 nm for the nanostructured films obtained under considered technological conditions can be regarded as optimum for the detection of alcohol (ethyl and isopropyl) vapors.

The response of the system is demonstrated to correlate well with the light absorption coefficient. Light with wavelengths shorter than 400 nm (i.e. in the interval close to ultraviolet) should be used in order to substantially affect the parameters of gas-sensitive structures.

1. Y. Sato, R. Tokumaru, E. Nishimura, P. Song, Yu. Shigesato, K. Utsumi, and H. Iigusa, J. Vac. Sci. Technol. A **23**, 1167 (2005).
2. G. Korotcenkov, Mater. Sci. Eng: B **139**, 1 (2007).
3. B.R. Eggins, *Biosensors: An Introduction* (Wiley, Chichester, 1996).
4. *An Introduction to Bioanalylical Sensors Techniques in Analytical Chemistry*, edited by A.J. Cunningham (Wiley, Chichester, 1996).
5. *Gas Sensors Principles, Operation, and Developments*, edited by G. Sberveglieri (Kluwer, Dordrecht, 1992).
6. *Semiconductor Sensors in Physico-Chemical Studies: Handbook of Sensors and Actuators*, edited by L.Y. Kupriyanov (Elsevier, Amsterdam, 1996).
7. S.Y. Yurish, *Digital Sensors and Sensor Systems: Practical Design* (IFSA, Barcelona, 2011).
8. A. Ayeshamariam, M. Bououdina, and C. Sanjeeviraja, Mater. Sci. Semicond. Process. **16**, 686 (2013).
9. L.A. Obvintseva, Ross. Khim. Zh. **52**, 113 (2008).
10. S.I. Rembeza, E.S. Rembeza, T.V. Svistova, and O.I. Borsyakova, Fiz. Tekh. Poluprovodn. **40**, 57 (2006).
11. S.I. Rembeza, Yu.V. Shmatova, T.V.Svistova, E.S. Rembeza, and N.N.Koshelev, Fiz. Tekh. Poluprovodn. **46**, 1213 (2012).
12. S.K. Tripathy, B.P. Hota, and V.S. Jahnavy, Zh. Nano-Electron. Fiz. **5**, 04055 (2013).
13. S.I. Rembeza, P.E. Voronov, B.M. Sinelnikov, and E.S. Rembeza, Fiz. Tekh. Poluprovodn. **45**, 1538 (2011).
14. D.I. Bilenko, O.Ya. Belobrovaya, E.A. Zharkova, D.V. Terin, and E.I. Khasina, Fiz. Tekh. Poluprovodn. **39**, 834 (2005).
15. O.I. Bomk, L.G. Il'chenko, V.V. Il'chenko, A.M. Pinchuk, V.M. Pinchuk, G.V. Kuznetsov, V.I. Strykha, Sensor. Actuat. B **62**, 131 (2000).
16. R. Balasundaraprabhua, E.V. Monakhova, N. Muthukumarasamyb, O. Nilsena, and B.G. Svenssona, Mater. Chem. Phys. **114**, 425 (2009).
17. Dewei Chu, Yu Ping Zeng, Dongliang Jiang, and Yo. Masuda, Sensor. Actuat. B **137**, 630 (2009).
18. Zhizhong Yuan, Dongsheng Li, Minghua Wang, Peiliang Chen, Daoren Gong, Peihong Cheng, and Deren Yang, Appl. Phys. Lett. **92**, 121908 (2008).
19. H.B. Huo, C. Wang, F.D. Yan, H.Z. Ren, and M.Y. Shen, J. Nanosci. Nanotechnol. **9**, 4817 (2009).
20. L.G. Il'chenko, A.A. Chuiko, V.V. Lobanov, and V.V. Il'chenko, in *Technical Digest of the 18th International Vacuum Nanoelectronics Conference (IVNC 2005)* (Oxford, 2005), p. 200.
21. A.I. Belyaeva, A.A. Galuza, and S.N. Kolomiets, Fiz. Tekh. Poluprovodn. **38**, 1050 (2004).
22. O.I. Barchuk, A.A. Goloborodko, V.N. Kurashov, Y.A. Oberemok, and S.N. Savenkov, Proc. SPIE **6254**, 62540W (2006).
23. O.I. Barchuk, T.V. Molebna, A.G. Chumakov, V.N. Kurashov, and V.V. Marjenko, Proc. SPIE **2648**, 62540W (2006).
24. A.A. Goloborodko, M.V. Epov, L.Y. Robur, and T.V. Rodionova, Zh. Nano-Electron. Fiz. **6**, 02002 (2014).
25. H. Fujiwara, *Spectroscopic Ellipsometry. Principles and Applications* (Wiley, Chichester, 2007).
26. L.A. Golovan', V.Yu. Timoshenko, and P.K. Kashkarov, Usp. Fiz. Nauk **177**, 619 (2007).
27. G.E. Jellison, T.E. Haynes, and H.H. Burke, Opt. Mater. **2**, 105 (1993).
28. A.A. Goloborodko, Zh. Nano-Electron. Fiz. **5**, 03048 (2013).
29. N.S. Goloborodko, V.M. Telega, and V.V. Il'chenko, in *Abstratcts of the 8th International Scientific Conference "Electronics and Applied Physics"* (Kyiv, 2012), p. 94.
30. *Handbook of Chemical and Biological Sensors*, edited by R.F. Taylor and J.S. Schultz (IOP Publishing House, Bristol, 1996).
31. V.V. Bolotov, V.E. Roslikov, E.A. Kurdyukova, A.V. Krivozubov, Yu.A.Sten'kin, and D.V. Cheredov, Fiz. Tekh. Poluprovodn. **46**, 109 (2012).

32. A. Fort, M. Mugnaini, S. Rocchi, M.B. Serrano-Santos, V. Vignoli, and R. Spinicci, Sensor. Actuat. B **124**, 245 (2007).
33. O.M. Lovvik, S. Diplas, A. Romanyuk, and A. Ulyashin, Appl. Phys. **115**, 083705 (2014).
34. N.S. Goloborodko and V.V. Ilchenko, Visn. Kyiv. Univ. Ser. Fiz. Mat. Nauky, No. 3, 296 (2012).
35. M.G. Nakhodkin, Y.S. Musatenko, and V.N. Kurashov, Proc. SPIE **3402**, 333 (1998).
36. A.O. Goloborodko, V.I. Grygoruk, M.M. Kotov, V.N. Kurashov, D.V. Podanchuk, and N.S. Sutyagina, Ukr. Fiz. Zh. **53**, 946 (2008).
37. P.N. Krylov, R.M. Zakirova, and I.V. Fedotova, Fiz. Tekh. Poluprovodn. **47**, 1421 (2013).
38. A.M. Gulyaev, Van Le Van, O.B. Sarach, and O.B. Mukhina, Fiz. Tekh. Poluprovodn. **42**, 742 (2008).
39. S.I. Rembeza, N.N. Koshelev, E.S. Rembeza, T.V. Svistova, Yu.V. Shmatova, and Gang Xu, Fiz. Tekh. Poluprovodn. **45**, 612 (2011).

Received 12.06.15.
Translated from Ukrainian by O.I. Voitenko

В.А. Виниченко, В.В. Бученко, Н.С. Голобородько, В.В. Лендел, О.Є. Лушкін, В.М. Телега

ОПТИЧНІ ТА ЕЛЕКТРОФІЗИЧНІ ВЛАСТИВОСТІ ГЕТЕРОСТРУКТУРИ 95% $In_2O_3 + 5\%$ SnO_2/ns-Si

Р е з ю м е

У роботі розглянуто оптичні та електрофізичні властивості гетероструктур 95% $In_2O_3 + 5\%$ SnO_2/ns-Si з товщиною плівок 6 та 12 нм, що наносились методом магнетронного розпилення на структуровану поверхню кремнію. Показано, що для плівки товщиною 6 нм характерна наявність декількох піків оптичного поглинання, тоді як у структурі з товщиною 12 нм в тому ж спектральному діапазоні ці максимуми відсутні. Визначено вплив газового середовища та оптичного випромінювання на електрофізичні властивості структур 95% $In_2O_3 + 5\%$ SnO_2/ns-Si та показано, що відгук досліджуваних структур на газове середовище пов'язаний з діелектричною проникністю адсорбату. Результати даного дослідження можна застосовувати при розробці резистивних газових сенсорів на основі плівок 95% $In_2O_3 + 5\%$ SnO_2/ns-Si.